Assessment of Negative Sequence Currents for Generators Connected to 345-kV Asymmetrical Transmission Lines from Measurement Data

Chi-Jui Wu and Ping-Heng Ho

Abstract**—**This paper is used to evaluate the negative sequence currents (NSC) of two generators in a generation plant, which are connected to the power pool through four asymmetrical 345-kV transmission lines. The two generators are located at the southern end of the Taiwan Power (Taipower) grid. These generators are very important to the system and provide base-period generation power. The simulation results by using PSS/E and EMTP are checked with the values from the wide area measurement system (WAMS). It can be observed that the factors such as parallel operations, lengths, current directions, and co-towered conditions of transmission lines will affect the values of NSC. The arrangement of conductors on the same tower in RST-R'S'T' or RST-T'S'R' configuration will have significant effects on the NSC values. This study estimates whether the generators need to reduce loading owing to the NSC to protect the generators. The study results give important information about generators connected to parallel asymmetrical transmission lines.

Keywords—Asymmetrical transmission lines, EMTP, Negative Sequence Current, PSS/E, Unbalance power system.

I. INTRODUCTION

The damages to generators by negative sequence currents (NSC) from the asymmetrical transmission lines depend on the levels of unbalanced conditions. The damages will not only reduce generator lifetime, but also increase system loss. The NSC may induce double-frequency currents in the rotor surface, retaining ring, slow wedge, and field winding. Then, the short period dangerous temperature in windings may be induced by abnormal rotor current [1-2]. There are articles describing the three-phase unbalanced systems [3]. The study about EHV double-circuit untransposed transmission lines and field measurements under different conditions were given [4]. The definitions of voltage unbalance to understand the implications to use were reviewed [5]. A simple and approximated method for assessing the NSC in EHV lines was described [6]. The three-phase unbalanced systems with unbalanced loads supplied from a three-wire line were dealt with, and the current was decomposed into three different components [7]. A mitigation technique was presented to reduce current unbalance in heavily loaded multi-circuit power lines [8]. The method to detect the NSC and properly apply relays to protect machines under system fault conditions was given [9]. A methodology using a utility's existing software was used in the estimation of NSC injected into utility generators [10]. A solution method was given to formulate a multiphase power flow model and state estimation for distribution systems [11]. A new measurement procedure based on neural networks was presented for the estimation of harmonic powers and current/voltage symmetrical components [12]. The measurements and simulation studies for the power flows and NSC before and after the outage of major transmission systems were compared [13].

In the transmission system of the Taiwan Power Company (Taipower), the RST-T'S'R' arrangement is used to reduce the unbalanced currents on the 345-kV double-circuit long distance untransposed transmission lines. However, single-circuit lines may be used in system maintenance periods. By the way, the RST- R'S'T' arrangement may be used under special operation conditions. It is possible that the NSC may increase by using single-circuit lines instead of double-circuit lines.

To evaluate the NSC level from four untransposed transmission lines, this study presented a useful methodology by using the PSS/E for balanced load flow calculation and the EMTP for three-phase calculation. At first, the line parameters were calculated by EMTP, and verified with the line data in PSS/E. Then according to the results of the balanced power flow, which was calculated by PSS/E, the three-phase power flow was checked by EMTP [14-15]. And the calculated data of the PSS/E and EMTP were corrected by measured results of WAMS in the N-0 and N-1 conditions [16-17]. Finally, the balanced and three-phase currents of the generation plant in N-2 and N-3 out-linking circuit conditions were calculated by PSS/E and EMTP. It is to obtain the NSC situations in different operation conditions. The NSC and the longest permissible withstanding operation time of the generator was estimated.

II. UNBALANCED POWER TRANSMISSION SYSTEM

2.1 Taiwan power system

The Taiwan power (Taipower) network is a medium-sized system with longitudinal structure, covering 400-km distance from north to south. The highest voltage level of transmission lines is 345-kV. Usually it can be divided into four areas as northern, central, southern, and eastern region.

Manuscript received on April 8, 2011.
Chi-Jui Wu and Ping-Heng Ho are with the Department of Electrical Engineering, National Taiwan University of Science and Technology. Taipei, Taiwan (cjwu@mail.ntust.edu.tw).

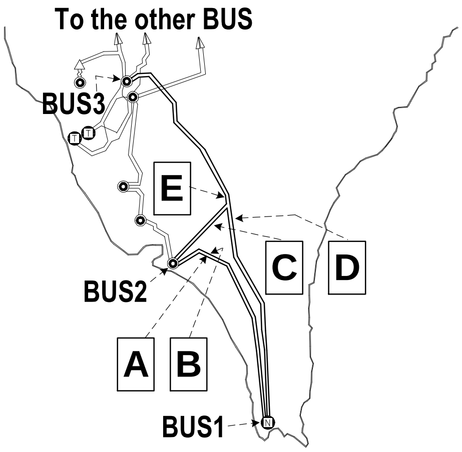

Fig. 1. The 345-kV transmission lines in the southern Taipower network.

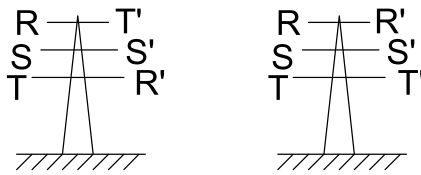

(a) (b)

Fig. 2. The conductor space arrangement (a) non-perfectly symmetrical RST-T'S'R', (b) asymmetrical RST-R'S'T'.

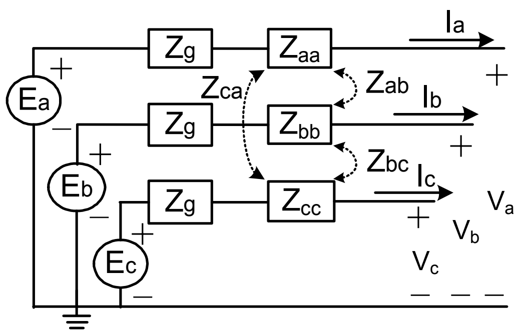

Fig. 3. Three-phase balanced source and untransposed transmission lines.

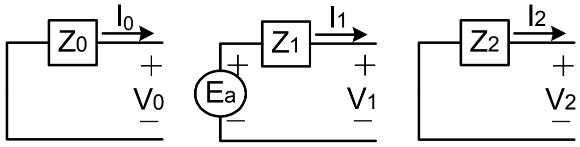

Fig. 4 Voltage sources in sequence networks.

In 2007, the generation capacity and the system peak load were 38,082-MW and 32,791-MW, respectively. The generation capacity ratio of the northern, central, southern, and eastern region was 31%, 32.4%, 36.4%, and 0.2%, respectively. The northern, central, southern, and eastern region occupied, respectively, 42.97%, 26.57%, 29.15%, and 1.31% of the total system peak load. Since the unbalance between generation and load in the northern region, electric power should be delivered from the southern region to the northern region. The system under study is shown in Fig. 1, where BUS 1 of a large generation station is located at the southern tip of the Taiwan. BUS 1 is connected to the power grid by four parallel and long distance 345-kV transmission circuits. The data of the Taipower system is listed in Appendix.

2.2 Asymmetrical Transmission Lines

If three-phase transmission line conductors are symmetrically spaced in a triangular configuration, the distance between each conductor is the same, which can reduce the unbalanced currents. Considering the difficulty in the construction of the Taipower transmission network, the double-circuit lines are co-towered and untransposed. The non-perfectly symmetrical RST-T'S'R' arrangement, as shown in Fig. 2(a), is used to reduce the unbalanced current. However, in some maintenance conditions, the asymmetrical RST-R'S'T' arrangement, as shown in Fig. 2(b), may be used. The current direction of the RST circuit may be same or different with that of the R'S'T' or T'S'R' circuit.

2.3 Sequence network

In analyzing unbalanced three-phase circuits, the method of symmetrical components is usually used [20]. A three-phase circuit with generator impedances Z_g, transmission circuit self impedances Z_{aa}, Z_{bb}, and Z_{cc}, respectively, and mutual impedances Z_{ab}, Z_{bc}, and Z_{ca}, respectively, is shown in Fig. 3. The generator neutral point is directly grounded.

The synchronous machine generates balanced three-phase internal voltages expressed by phasors as

$$E^{abc} = \begin{bmatrix} 1 \\ a^2 \\ a \end{bmatrix} E_a \tag{1}$$

where

$$a = -\frac{1}{2} + j\frac{\sqrt{3}}{2} \tag{2}$$

According to the Kirchhoff's voltage law, the line-to-ground voltages are

$$\begin{aligned} V_a &= E_a - Z_g I_a - Z_{aa} I_a - Z_{ab} I_b - Z_{ac} I_c \\ V_b &= E_b - Z_g I_b - Z_{ba} I_a - Z_{bb} I_b - Z_{bc} I_c \\ V_c &= E_c - Z_g I_c - Z_{ca} I_a - Z_{cb} I_b - Z_{cc} I_c \end{aligned} \tag{3}$$

Using the sequence component approach, we have

$$\begin{bmatrix} V_a \\ V_b \\ V_c \end{bmatrix} = \begin{bmatrix} E_a \\ E_b \\ E_c \end{bmatrix} - Z^{abc} \begin{bmatrix} I_a \\ I_b \\ I_c \end{bmatrix} \tag{4}$$

where

$$Z^{abc} = \begin{bmatrix} Z_g + Z_{aa} & Z_{ab} & Z_{ac} \\ Z_{ba} & Z_g + Z_{bb} & Z_{bc} \\ Z_{ca} & Z_{cb} & Z_g + Z_{cc} \end{bmatrix} \tag{5}$$

Then

$$A\begin{bmatrix} V_0 \\ V_1 \\ V_2 \end{bmatrix} = A\begin{bmatrix} 0 \\ E_a \\ 0 \end{bmatrix} - Z^{abc} A\begin{bmatrix} I_0 \\ I_1 \\ I_2 \end{bmatrix} \tag{6}$$

where

$$A = \begin{bmatrix} 1 & 1 & 1 \\ 1 & a^2 & a \\ 1 & a & a^2 \end{bmatrix} \tag{7}$$

Multiplying both sides of (6) by A^{-1}, we get

$$\begin{bmatrix} V_0 \\ V_1 \\ V_2 \end{bmatrix} = \begin{bmatrix} 0 \\ E_a \\ 0 \end{bmatrix} - A^{-1} Z^{abc} A\begin{bmatrix} I_0 \\ I_1 \\ I_2 \end{bmatrix} \tag{8}$$

Then

$$\begin{bmatrix} V_0 \\ V_1 \\ V_2 \end{bmatrix} = \begin{bmatrix} 0 \\ E_a \\ 0 \end{bmatrix} - Z^{012}\begin{bmatrix} I_0 \\ I_1 \\ I_2 \end{bmatrix} \tag{9}$$

where

$$Z_{012} = \begin{bmatrix} Z_{s0} + 2Z_{m0} & Z_{s2} - Z_{m2} & Z_{s1} - Z_{m1} \\ Z_{s1} - Z_{m1} & Z_{s0} - Z_{m0} & Z_{s2} + 2Z_{m2} \\ Z_{s2} - Z_{m2} & Z_{s1} + 2Z_{m1} & Z_{s0} - Z_{m0} \end{bmatrix} \tag{10}$$

with

$$\begin{aligned} Z_{s0} &= \frac{1}{3}\left(Z_{aa} + Z_{bb} + Z_{cc}\right) \\ Z_{s1} &= \frac{1}{3}\left(Z_{aa} + aZ_{bb} + a^2 Z_{cc}\right) \\ Z_{s2} &= \frac{1}{3}\left(Z_{bc} + a^2 Z_{ca} + aZ_{ab}\right) \end{aligned} \tag{11}$$

and

$$\begin{aligned} Z_{m0} &= \frac{1}{3}\left(Z_{bc} + Z_{ca} + Z_{ab}\right) \\ Z_{m1} &= \frac{1}{3}\left(Z_{bc} + aZ_{ca} + a^2 Z_{ab}\right) \\ Z_{m2} &= \frac{1}{3}\left(Z_{bc} + a^2 Z_{ca} + aZ_{ab}\right) \end{aligned} \tag{12}$$

The three independent sequence networks are revealed in Fig. 4.

2.4 Transmission Lines Model

The LINE CONSTANTS supporting routines of EMTP could be used to solve the steady-state problems with complicated coupling effects under the power frequency [21]. According to the data about tower types, geometrical space, line material, conductor specification, and length, the transmission line matrices [R], [L], and [C] are calculated.

2.5 The NSC expression

The expression of NSC is based on the IEEE Std C37.102-2006 [22] and the IEEE Std C50.13-2005 [23]. The normalized NSC of transmission lines is defined as

$$\mathrm{I}_{2,\mathrm{L}} = \frac{\text{Negative sequence current}}{\text{Positive sequence current}} \tag{13}$$

For the generators, it is defined as

$$\mathrm{I}_{2,\mathrm{G}} = \frac{\text{Negative sequence current}}{\text{Rated stator current}} \tag{14}$$

2.6 Ability of a generator to withstand unbalanced current

The ability of a generator to withstand permissible continuous NSC is also specified both in the IEEE Std C37.102-2006 and IEEE Std C50.13-2005. According to the IEEE Std C37.102-2006, the percentage permissible withstanding continuous NSC of generators from 351-MVA to 1,250-MVA is given by

$$I_2 = 8 - (MVA - 350)/300 \quad \% \tag{15}$$

In this study, the generator capacity is 1,057.5-MVA, and then the permissible withstanding continuous NSC is 5.64%. The ability of a generator to accommodate NSC is described by

$$K = I_2^2 t = 10 - (0.00625)(MVA - 800) \tag{16}$$

The K value of the generators in this study is 8.39.

2.7 The NSC relay setting

The picking up alarm and tripping settings of the NSC relay in this study are set to be 80% and 90% of the permissible withstanding continuous NSC values, respectively. The dial time setting of the NSC relay of generators in this study is set to be 90% of the ability to withstand NSC. Each value is rounded to integer. So that, in this study, the alarm is picked up when $\mathrm{I}_{2,\mathrm{G}}$ reaches 4%. The tripping is picked up and the dial time is started when $\mathrm{I}_{2,\mathrm{G}}$ reaches 5%. The tripping signal is started when K reaches 7. It is summarized as the following

$$\begin{aligned} I_{2,G(alarm)} &= 4\% \\ I_{2,G(trip)} &= 5\% \\ K_{(trip)} &= 7 \end{aligned} \tag{17}$$

III. The WAMS Monitoring System

The technique of the wide area measurement system (WAMS) came from the theory of sequence components for distance protection relay [24-29]. In order to monitor the dynamic and transient behaviors of the 345-kV network, the Taipower had installed 10 WAMS units. Fig. 5 shows the schematic arrangement of the WAMS hardware. The functions of the WAMS include the power system real-time monitoring, the analysis of dynamical behaviors, fault recording, and the steady state analysis of phasor recording.

The block diagram of the synchronous phasor measurement unit (PMU) in the WAMS is shown in Fig. 6. The PMU is composed of the signal conditioning unit (SCU), the measurement unit (MU), and the satellite signal synchronizing unit (SSU). To acquire the phase angles and bus frequency data among substations, a global reference is needed. The time stamp of the PMU is the same as the global positioning system (GPS). The data from different PMU is delivered to the central control unit by optical fibers. The data are then computed by using the discrete Fourier transform algorithm on a common time base. The symmetrical components of voltages and currents are computed from the instantaneous values.

In this study, the data was adopted from the four out-linking circuits at BUS 1 and the inter-linking circuit between BUS 2 and BUS 3, as shown in Fig. 1. The values from the WAMS are used to correct the models and parameters in the EMTP.

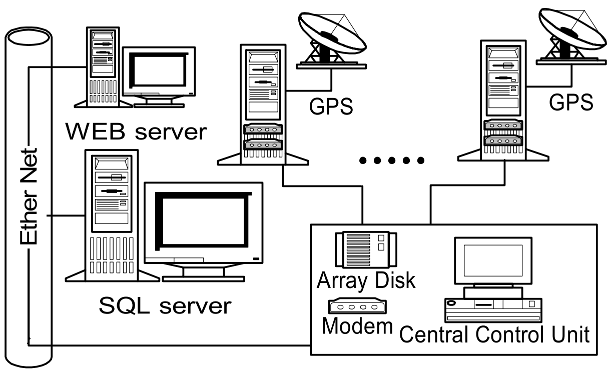

Fig. 5. Schematic arrangement of the WAMS hardware.

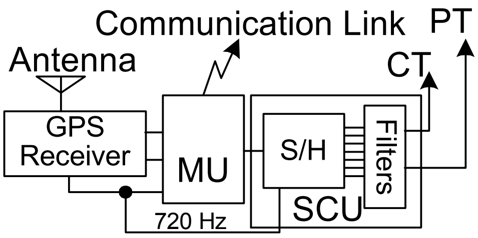

Fig. 6. Block diagram of synchronous phasor measurement system.

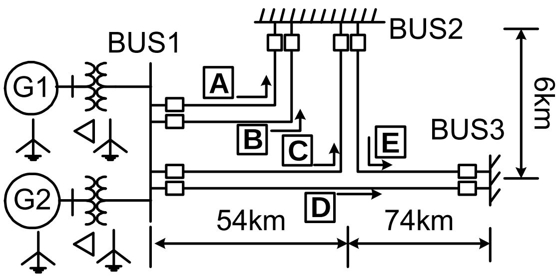

Fig. 7. One-line diagram of the 345-kV transmission system (arrow indicates current direction in the N-0 condition).

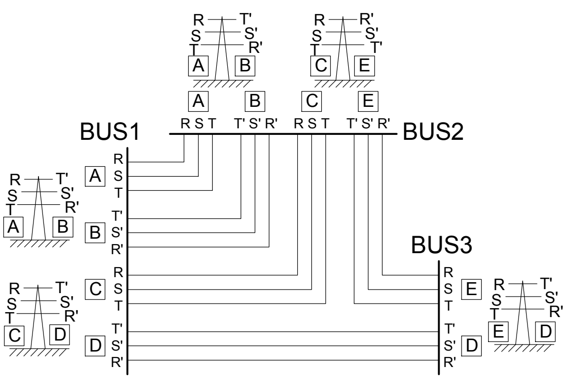

Fig. 8. Conductor arrangement of the transmission lines.

IV. Transmission Line Model Verified

The transmission line models include resistance, reactance, and conductance of the positive-sequence and negative-sequence circuits and the mutual inductance. To verify the models, the simulation results of PSS/E and EMTP are compared with that measured by WAMS.

4.1 System scheme

Figure 7 shows the one-line diagram of the study system, where four circuits, A, B, C, and D, out-link from BUS 1. Circuit E connects BUS 2 and BUS 3. The current directions of circuits C and E are different. Fig. 8 shows the conductor arrangement of the five circuits. Circuits A and B are co-towered and have same current direction. The conductors of circuits A and B are in RST-T'S'R' arrangement. Circuits C, D, and E are partially co-towered. The co-tower conductors of circuits C and D, circuits C and E, and circuits D and E are, respectively, in RST-T'S'R', RST-R'S'T', and T'S'R'-RST arrangement. The tower data and line material of the five circuits are listed in Appendix. The transformers data is also given in Appendix.

4.2 Operation cases

Since circuits A, B, C, and D are the four out-linking lines from BUS 1, they have significant effects on NSC. The N-0 condition means that the four out-linking circuits are used normally. The N-1, N-2, N-3, and N-4 conditions mean that 1, 2, 3, and 4 circuits, respectively, have been opened. Then, according to the conditions of circuits being opened, there are 32 study cases.

TABLE I
COMPARISON OF CALCULATION DATA FROM EMTP AND PSS/E DATA USED BY UTILITY

Circ-uit	Method	R1+jX1 (Ω)	R0+jX0 (Ω)	Q0 (MVA)	Q1 (MVA)	R00+ jX00 (Ω)
A	EMTP Model	1.014 +j17.57	8.37 +j48.51	19.27	36.26	7.35 +j24.93
	PSS/E	1.029 +j17.99	9.59 +j51.77	22.7	22.7	7.95 +j26.85
B	EMTP Model	1.014 +j17.57	8.37 +j48.51	19.27	36.26	7.35 +j24.93
	PSS/E	1.029 +j17.99	9.59 +j51.77	22.7	22.7	7.95 +j26.85
C	EMTP Model	1.055 +j18.29	8.71 +j50.5	20.02	37.74	7.65 +j25.95
	PSS/E	0.92 +j19.16	9.72 +j52.18	30.7	30.7	7.72 +j24.26
D	EMTP Model	2.286 +39.37	19.04 +j109.1	43.24	81.24	16.74 +j56.22
	PSS/E	2.76 +j40.71	11.8 +j106.7	67.97	67.97	6.86 +j39.26
E	EMTP Model	1.416 +j24.5	11.71 +j67.69	26.84	50.55	10.29 +j34.81
	PSS/E	1.82 +j25.07	9.26 +j73.8	41.9	41.9	4.29 +j24.56

TABLE II
OPERATION CONDITION OF CIRCUITS FOR VERIFICATION

Case	Circuit					WAMS	
	A	B	C	D	E	Date	Time
0-A	X	X	X	X	X	2007.08.02	16:50:00
0-B	X	X	X	X	—	2007.03.27	04:20:00
1-1A	—	X	X	X	X	2007.05.21	02:48:00
1-2A	X	—	X	X	X	2007.02.12	08:00:00
1-3A	X	X	—	X	X	2007.05.18	06:24:00
1-4A	X	X	X	—	X	2006.10.11	07:52:00

Note: “X” circuits closed, “—” circuits opened

TABLE III
COMPARISON OF PHASE CURRENT (KA, RMS) IN PSS/E AND WAMS

Case		Method	Circuit				
			A	B	C	D	E
N-0	0-A	WAMS	0.8	0.81	0.76	0.65	0.46
		PSS/E	0.81	0.81	0.76	0.64	0.46
	0-B	WAMS	0.79	0.8	0.75	0.8	—
		PSS/E	0.77	0.77	0.73	0.77	
N-1	1-1A	WAMS	—	1.19	1.15	0.79	0.38
		PSS/E		1.18	1.11	0.75	0.38
	1-2A	WAMS	1.17	—	1.16	0.79	0.36
		PSS/E	1.19		1.11	0.75	0.38
	1-3A	WAMS	1.18	1.2	—	0.73	0.37
		PSS/E	1.16	1.16		0.74	0.38
	1-4A	WAMS	1.05	1.07	0.96	—	0.65
		PSS/E	1.04	1.04	0.97		0.68

Note: “—” circuits opened

TABLE IV
COMPARISION OF $I_{2,L}$ (%) FROM EMTP AND WAMS

Case		Method	Circuit				
			A	B	C	D	E
N-0	0-A	WAMS	0.47	1.16	1.93	1.71	1.33
		EMTP	0.76	1.31	1.97	3.39	2.79
	0-B	WAMS	0.67	1.19	1.53	3.65	—
		EMTP	0.42	0.83	0.82	6.27	
N-1	1-2A	WAMS	—	3.73	0.86	0.96	1.59
		EMTP		4.78	1.42	2.94	2.16
	1-3A	WAMS	3.01	—	0.78	1.55	2.5
		EMTP	4.55		1.58	2.73	2.16
	1-4A	WAMS	2.06	1.38	—	1.94	1.15
		EMTP	1.04	1.42		6.32	0.66
	1-5A	WAMS	0.4	0.78	4.97	—	4.98
		EMTP	1.01	1.08	5.91		9.04

Note: “—” circuits opened

4.3 Model verification

(a)Line parameters: According to the data in Appendix, it is calculated by the LINE CONSTANTS routine of EMTP. TABLE I shows the comparison of the calculation data of EMTP and the system data of the PSS/E used by Taipower. In TABLE I, the difference between data is acceptable.

(b) System verification: Several system measurement records of the WAMS can be used. TABLE II gives six operation cases, where one of the five circuits is opened.

(c) Comparison of PSS/E with WAMS: The simulation currents from PSS/E after adjusting the output of generators and the measurement currents from WAMS are approximated, as listed in TABLE III. The results of PSS/E are acceptable.

(d) Comparison of EMTP with PSS/E: According to the balanced currents of PSS/E, the three-phase currents of EMTP were calculated by adjusting the voltage sources in EMTP.

(e) Comparison of EMTP with WAMS: Then the three-phase currents are then converted to the sequence currents as listed in TABLE IV. The currents of EMTP and that from WAMS are approximated. The system data in EMTP is reasonable. The NSC of other study cases could be estimated.

V. NSC ESTIMATION

The study cases are given in TABLE V with values of $I_{2,G}$ and $I_{2,L}$, and the longest permissible withstanding operation time of generators.

5.1 Conditions in full loading

In N-0 conditions, such as cases 0-A and 0-B, $I_{2,G}$ lies in 1.665% to 2.016%. The generators could be operated in full loading because $I_{2,G}$ is lower than 4%. In N-1 conditions, there are 8 cases, i.e., Case 1-1A to Case 1-4B, and $I_{2,G}$ lies in 1.952% to 3.297%. Then, the generators also could be operated in full loading. In N-2 conditions, there are four cases with co-towered arrangement. They are Case 2-1A, Case 2-1B, Case 2-6A, and Case 2-6B. In those cases, $I_{2,G}$ lies in 1.915% to 3.532%. The generators also could be operated in full loading. Also in the N-2 conditions at different towers and with circuit D being opened, such as Case 2-3A, Case 2-3B, Case 2-5A, and Case 2-5B, $I_{2,G}$ lies in 3.974% to 4.776%. The generators could be operated in full loading but need attention since $I_{2,G}$ is over the alarm value 4% but still lower than the tripping value 5%.

5.2 Conditions in reduced loading

(a)In the N-2 conditions at different towers and with the short lines being opened: The 60-km long circuit A or B and the 128-km long circuit D are closed. There are Case 2-2A, Case 2-2B, Case 2-4A, and Case 2-4B as shown in Fig. 9. The value of $I_{2,G}$ lies in 5.118% to 5.545%. Since it is larger than the tripping value 5%, the generators should not be operated in full loading or K will reach 7 after 37.98 minutes and the relay will then be tripped.

In the comparison of Case 2-2A with Case 2-2B, Case 2-2A uses circuit E to transmit power, which lets $I_{2,G}$ be smaller. It is because that circuit E could mitigate the unbalanced current of the circuit D. In the same reason, Case 2-4A also uses circuit E, and let $I_{2,G}$ be smaller.

TABLE V
$I_{2,G}$, $I_{2,L}$, AND LONGEST PERMISSIBLE WITHSTANDING OPERATION TIME OF GENERATORS

Condition	Case	$I_{2,G}$ (%)	$I_{2,L}$ (%) circuit A	B	C	D	E	Longest time (Min)
N-0	0-A	1.665	0.76	1.31	1.97	3.39	2.79	∞
	0-B	2.016	0.42	0.83	0.82	6.27	—	∞
N-1	1-1A	3.071	—	4.78	1.42	2.94	2.16	∞
	1-1B	3.297	—	4.44	0.54	4.93	—	∞
	1-2A	3.013	4.55	—	1.58	2.73	2.16	∞
	1-2B	3.233	4.29	—	0.65	4.96	—	∞
	1-3A	2.339	1.04	1.42	—	6.32	0.66	∞
	1-3B	2.733	0.71	0.73	—	7.94	—	∞
	1-4A	2.461	1.01	1.08	5.91	—	9.04	∞
	1-4B	1.952	0.3	0.65	5.38	—	—	∞
N-2	2-1A	3.532	—	—	3.64	3.33	5.44	∞
	2-1B	2.284	—	—	3.42	4.32	—	∞
	2-2A	5.383	—	4.94	—	6	3.19	40.26
	2-2B	5.545	—	4.8	—	6.63	—	37.98
	2-3A	4.776	—	4.76	4.32	—	10.42	∞
	2-3B	3.986	—	4.14	3.7	—	—	∞
	2-4A	5.188	4.76	—	—	5.89	1.64	43.38
	2-4B	5.352	4.56	—	—	6.67	—	40.74
	2-5A	4.715	4.5	—	4.34	—	10.54	∞
	2-5B	3.974	3.91	—	3.88	—	—	∞
	2-6A	2.492	3.45	2.61	—	—	9.35	∞
	2-6B	1.915	1.81	2.05	—	—	—	∞
N-3	3-1A	9.564	—	—	—	9	29.76	12.78
	3-1B	8.661	—	—	—	8.2	—	15.54
	3-2A	6.246	—	—	6.3	—	11.34	29.88
	3-2B	5.888	—	—	5.82	—	—	33.72
	3-3A	6.514	—	6.36	—	—	12.47	27.48
	3-3B	5.95	—	5.8	—	—	—	32.94
	3-4A	6.167	6.23	—	—	—	12.31	30.66
	3-4B	5.776	5.69	—	—	—	—	34.98
N-4	4-1A	—	—	—	—	—	—	—
	4-1B	—	—	—	—	—	—	—

Note: "—" circuits opened

(b) In the N-3 condition with the short lines being opened: In these conditions, only one circuit is connected to BUS 1. Fig. 10 shows Case 3-1A and Case 3-1B for study. The value of $I_{2,G}$ is 9.564% and 8.661%, respectively, which is larger than the tripping value 5%. The generators should not be operated in full loading or K will reach 7 after 12.78 minutes and trip the generators. It is suggested to reduce the generator loading until $I_{2,G}$ is lower than the alarm value 4%. Case 3-1A only uses the 128-km long circuit D, which is partially co-towered with the 74-km long circuit E in T'S'R'-RST arrangement. The two circuits have opposite current direction. It makes $I_{2,G}$ be larger than the relay tripping value 5%. The $I_{2,G}$ of Case 3-1A is higher than that of Case 3-1B.

(c) In N-3 conditions with long lines being opened: The long circuit D is opened. Six cases are given in Fig. 11. The value of $I_{2,G}$ lies in 5.776% to 6.246%, which is larger than the tripping value 5%. If the generators are operated in full loading, K will reach 7 after 29.88 minutes.

Both Case 3-2A and Case 3-2B use the 60-km circuit C. In Case 3-2A, circuit C is partially co-towered with circuit E in RST-R'S'T' arrangement and with opposite current direction. However, the co-towered part is only 6-km long. Also, in Case 3-2A, the non co-towered part of circuit E is 74-km. So the $I_{2,G}$ of Case 3-2A is higher than that of Case 3-2B.

Both Case 3-3A and Case 3-3B use the 60-km circuit B. However, Case 3-3A also uses the 80-km circuit E, which makes the $I_{2,G}$ of Case 3-3A be higher than that of Case 3-3B. In Case 3-2A, circuit C and partial circuit E are co-towered about 6-km and in RST-R'S'T' arrangement, which could mitigate NSC, but Case 3-3A has no co-towered circuit. The $I_{2,G}$ of Case 3-2A is lower than that of Case 3-3A. Both Case 3-4A and Case 3-4B use the 60-km circuit A. However, Case 3-4A also uses the 80-km circuit E, which makes the $I_{2,G}$ of Case 3-4A be higher than that of Case 3-4B.

The $I_{2,G}$ of Case 3-3B is higher than that of Case 3-4B, owing to the different arrangement in conductors. Both Case 3-3A and Case 3-4A use circuit E. The NSC produced from circuit E is similar. The $I_{2,G}$ of Case 3-3A is higher than that of Case 3-4A, owing to the different arrangement in the conductors.

(d) In N-4 condition: When the four out-linking circuits are opened, such as Case 4-1A and Case 4-1B, it is impossible to transmit the power. This study does not discuss these conditions.

The summary about $I_{2,G}$ and the suggestion to the operation of generators are given in TABLE VI.

(1) In N-0 and N-1 conditions: If $I_{2,G}$ is lower than the relay alarm value 4%, the generators can be operated at full load.

(2) In N-2 conditions:

A. In same tower cases: If $I_{2,G}$ is close to the relay alarm value 4% in the same tower cases, the generators can be operated at full load but it has to pay attention.

B. In different tower cases: If $I_{2,G}$ reaches the relay alarm value 4% in the different tower cases with the long distance circuit D being opened, the generators can be operated at full load. If one of circuits A, B, or C is opened, $I_{2,G}$ will be larger than the relay tripping value 5%, so that the generators should not be operated at full load. It is recommended to let $I_{2,G}$ be lower than 4% by reducing the loading of generators.

(3) In the N-3 conditions: If $I_{2,G}$ is larger than the relay tripping value 5%, the generators should not be operated at full load. It is also recommended to let $I_{2,G}$ be lower than 4% by reducing the loading of generators.

(4) In the practical operation rules of Taipower, the loading of each generator is reduced to 75% in the N-2 conditions. This is more conservative than the results in this paper.

TABLE VI
SUMMARY OF $I_{2,G}$ AND SUGGESTIONS TO GENERATORS

<table>
<tr><th>Conditions</th><th colspan="2">Co-towered or not</th><th>$I_{2,G}$ (%)</th><th>Generators in full loading or not</th></tr>
<tr><td>N-0</td><td colspan="2">—</td><td>1.665~2.016</td><td>Yes</td></tr>
<tr><td>N-1</td><td colspan="2">—</td><td>1.952~3.297</td><td>Yes</td></tr>
<tr><td rowspan="3">N-2</td><td colspan="2">Yes</td><td>1.915~3.532</td><td>Yes. Need attention.</td></tr>
<tr><td rowspan="2">No</td><td>Circuit D opened</td><td>3.974~4.776</td><td>Yes. Need attention if $I_{2,G}$ is over 4%.</td></tr>
<tr><td>Circuit A, B, or C opened</td><td>5.118~5.545</td><td>No. To reduce loading until $I_{2,G}$ is lower than 4%.</td></tr>
<tr><td>N-3</td><td colspan="2">—</td><td>5.776~9.564</td><td>No. To reduce loading until $I_{2,G}$ is lower than 4%.</td></tr>
</table>

VI. CONCLUSIONS

To examine the NSC from five transmission circuits, this study presented a comprehensive approach by using the simulation results from PSS/E and EMTP, and the measurement results from WAMS. The balanced load flow calculation by PSS/E and the unbalanced three-phase load flow calculation by EMTP are compared with the measurement by WAMS. The models and parameters established by the EMTP are approximated to the system data in PSS/E. The NSC cases were analyzed by EMTP and verified by the data from WAMS. The factors such as the length of circuits, the co-towered conditions, and the phasing configurations in RST-R'S'T' or RST-T'S'R' will affect the NSC. In some N-2 and N-3 conditions, NSC will be larger than the relay tripping value, and the generators should not be operated in full loading. To reduce the generator loading until NSC is lower than the relay alarm value is suggested. When generators are connected to the transmission system through parallel transmission circuits, it should examine the NSC values to ensure the safe operation of generators.

ACKNOWLEDGMENT

The paper is supported by the National Taiwan University of Science and Technology and National Science Council of Taiwan, project number, NSC 100-3113-E-194 -001 and 99-2221-E-011-147-MY3.

APPENDIX

A. System load

The peak load of Taipower system in 2007 was 32,791-MW. The North, Center, South, and East area occupied 42.97%, 26.57%, 29.15%, and 1.31%, respectively. The system load was listed in Table AI.

B. Conductor data

The standard type A 345-kV steel towers are used. The cross section of the 345-kV power line corridor is shown in Fig. AI. The resistance of the tower to ground is 20 ohms. The 795-MCM (26/7) ACSR/AW conductors are used. The radius of the conductor is 2.8143 cm.

C. 345-kV circuit

The characteristics of 345-kV conductors are listed in TABLE AII. The specification and length of the 345-kV circuits are listed in TABLE AIII. The DC resistor is 0.064907 ohm/km in 20 degrees Celsius. The bundling and skin effects are considered. The radius of the overhead grounded wire is 1.632 cm. Its DC resistor is 0.275 ohm/km in 20 degrees Celsius.

D. Transformer

Each 23.7/345-kV, Y-△ connected transformer consists of three single-phase units. The capacity of each single-phase unit is 336 MVA. The equivalent impedance, Zps, is 0.2289+j17.0256 ohm/phase. The exciting admittance is 273.43-j825.64 micro-Siemen/phase. In the open-circuit test data, there are 100% voltage, 0.075% current, and 170-kW loss. In the short-circuit test data, there are 14.4% impedance and 660-kW loss.

TABLE AI
SYSTEM LOAD (MW)

Area	Generation	Load	Balance	Line loss
Northern	10475	14335.1	-4031.2	171.1
Central	10940	8732.1	1969.7	264.1
Southern	12310	9663.2	2422.6	198.8
Eastern	80	428.1	-361.1	13
Total	33805	33158.5	0	647.1

TABLE AII
LINE PARAMETERS

Phase	Radius (cm)	DC Resistance (ohm/km)	Horiz (m)	V_{tower} (m)	V_{mid} (m)	Separ (cm)	Per Phase Conductor Number
R	1.408	0.064907	-7.05	34.35	30.35	40	4
S	1.408	0.064907	-7.4	25.45	21.45	40	4
T	1.408	0.064907	-7.8	16.5	12.5	40	4
R'	1.408	0.064907	7.8	16.5	12.5	40	4
S'	1.408	0.064907	7.4	25.45	21.45	40	4
T'	1.408	0.064907	7.05	34.35	30.35	40	4
0	0.816	0.275	-8	45.35	41.35	0	1
0	0.816	0.275	8	45.35	41.35	0	1

TABLE AIII
345-KV CONDUCTOR AND LENGTH

Circuit	Conductor	Length (km)
A	ACSR795Q/26	60
B	ACSR795Q/26	60
C	ACSR795Q	60
D	ACSR795Q	128
E	ACSR795Q	80

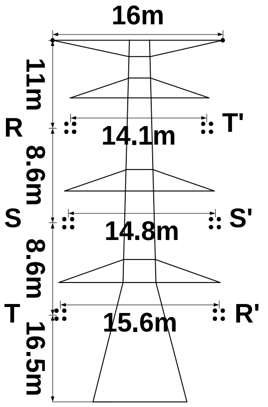

Fig. A1 Cross section of the 345-kV power line corridor.

REFERENCE

[1] W. H. Kersting, "Gauses and effect of unbalanced voltages serving an induction moter," *IEEE Trans. Industry Applications*, vol. 37, no. 1, pp. 165-170, Jan./Feb. 2001.

[2] G. Chicco, P. Postolache, and C. Toader, "Analysis of three-phase systems with neutral under distorted and unbalanced conditions in the symmetrical component-based framework," *IEEE Trans. Power Delivery*, vol. 22, no. 1, pp. 674-683, Jan. 2007.

[3] W. V. Lyon, "Reactive power and unbalanced circuits," *Electrical World*, vol. 75, no. 25, pp. 1417-1420, Jun. 1920.

[4] M. H. Hesse and J. Sabath, "EHV double-circuit untransposed transmission line-analysis and tests," *IEEE Trans. Power App. Sys.*, vol. PAS-90, issue 3, pp. 984-992, May 1971.

[5] P. Pillay and M. Manyage, "Definitions of voltage unbalance," *IEEE Power Engineering Review*, pp. 50-51, May 2001.

[6] M. M. Adibi, D. P. Milanicz, and T. L. Volkmann, "Asymmetry issues in power system restoration," *IEEE Trans. Power Systems*, vol. 14, no. 3, pp. 1085-1091, Aug. 1999.

[7] L. S. Czarnecki, "Power related phenomena in three-phase unbalanced systems," *IEEE Trans. Power Delivery*, vol. 10, no. 3, pp. 1168-1176, Jul. 1995.

[8] J. Ma and F. P. Dawalibi, "Analysis and mitigation of current unbalance due to induction in heavily loaded multicircuit power lines," *IEEE Trans. Power Delivery*, vol. 19, no. 3, pp. 1378-1383, Jul. 2004.

[9] J. E. Barkle and W. E. Glassburn, "Protection of generators against unbalanced current," *AIEE Trans. Part III*, vol. 72, pp. 282-285, 1953.

[10] S.-L. Chen, R.-J. Li, and P.-H. Hsi, "Traction system unbalance problem-analysis methodologies," *IEEE Trans. Power Delivery*, vol. 19, no. 4, pp. 1877-1882, Oct. 2004.

[11] A. P. S. Meliopoulos and F. Zhang, "Multiphase power flow and state estimation for power distribution systems," *IEEE Trans. Power Systems*, vol. 11, no. 2, pp.939-946, May 1996.

[12] F. J. Alcantara and P. Salmeron, "A new technique for unbalance current and voltage estimation with neural networks," *IEEE Trans. Power Systems*, vol. 20, no. 2, pp. 852-858, May 2005.

[13] Z. Emin and D. S. Crisford, "Negative phase-sequence voltages on E&W transmission system," *IEEE Trans. Power Delivery*, vol. 21, no. 3, pp. 1607-1612, Jul. 2006.

[14] Shaw Technologies, Inc., *PSS/E 30 Online Documentation*, August 2004.

[15] Leuven EMTP Center (LEC), *Alternative Transients Program (ATP) Rule Book*, July, 1987.

[16] J. A. Martinez, B. Gustavsen, and D. Durbak, "Parameter determination for modeling system transients-part I: overhead lines," *IEEE Trans. Power Delivery*, vol. 20, no. 3, pp. 2038-2044, Jul. 2005.

[17] A. Martinez, R. Walling, B. A. Mork, J. M.-Arnedo, and D. Durbak, "Parameter determination for modeling system transients-part III: transformers," *IEEE Trans. Power Delivery*, vol. 20, no. 3, pp. 2051-2062, Jul. 2005.

[18] W. D. C. Boaventura, A. Semlyen, M. R. Iravani, and A. Lopes, "Sparse network equivalent based on time-domain fitting," *IEEE Tran. Power Delivery*, vol. 17, no. 1, pp. 182-189, Jan. 2002.

[19] M. A.-Rahman, A. Semlyen, and M. R. Iravani, "Two-layer network equivalent for electromagnetic transients," *IEEE Tran. Power Delivery*, vol. 18, no. 4, pp. 1328-1335, Oct. 2003.

[20] H. Saadat, *Power System Analysis*, New York: McGraw-Hill, 1999.

[21] W. S. Meyer and T.-H. Liu, *Electro-Magnetic Transients Program (EMTP) Theory Book*, Bonneville Power Administration, Feb. 1986.

[22] *IEEE Guide for AC Generator Protection*, IEEE Standard C37.102-2006, Feb. 2007.

[23] *IEEE Standard for Cylindrical-Rotor 50Hz and 60 Hz Synchronous Generators Rated 10 MVA and Above*, IEEE Standard C50.13-2005, Feb. 2006.

[24] A. G. Phadke, T. Hlibka, M. Ibrahim, M. G. Adamiak, "A microcomputer based symmetrical component distance relay" in *Proc. 1979 IEEE Power Industry Computer Applications Conf.*, pp. 47-55.

[25] A. G. Phadke, M. Ibrahim, T. Hlibka, "Fundamental basis for distance relaying with symmetrical components", *IEEE Trans. Power App. Sys.*, vol. PAS-96, no. 2, pp. 635-646, 1977.

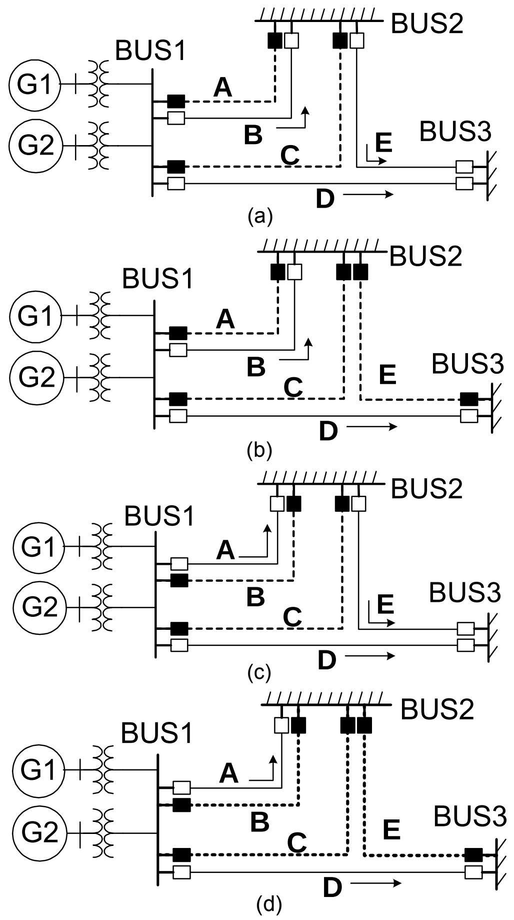

Fig. 9. N-2 conditions at different towers with short distance lines being opened (a) Case 2-2A (circuits A and C being opened), (b) Case 2-2B (circuits A, C, and E being opened), (c) Case 2-4A (circuits B and C being opened), (d) Case 2-4B (circuits B, C, and E being opened)

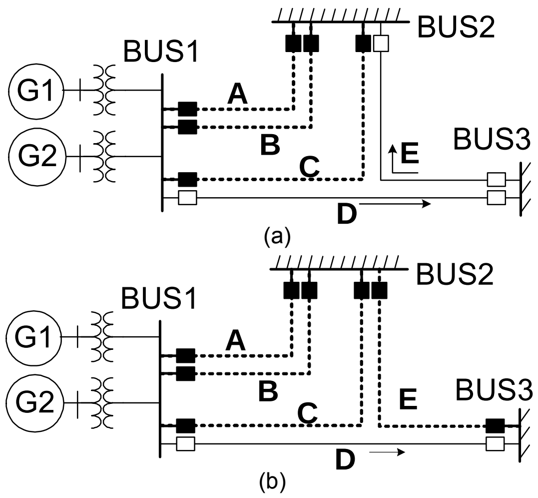

Fig. 10. N-3 conditions with short distance lines being opened (a) Case 3-1A (circuits A, B, and C being opened), (b) Case 3-1B (circuits A, B, C, and E being opened)

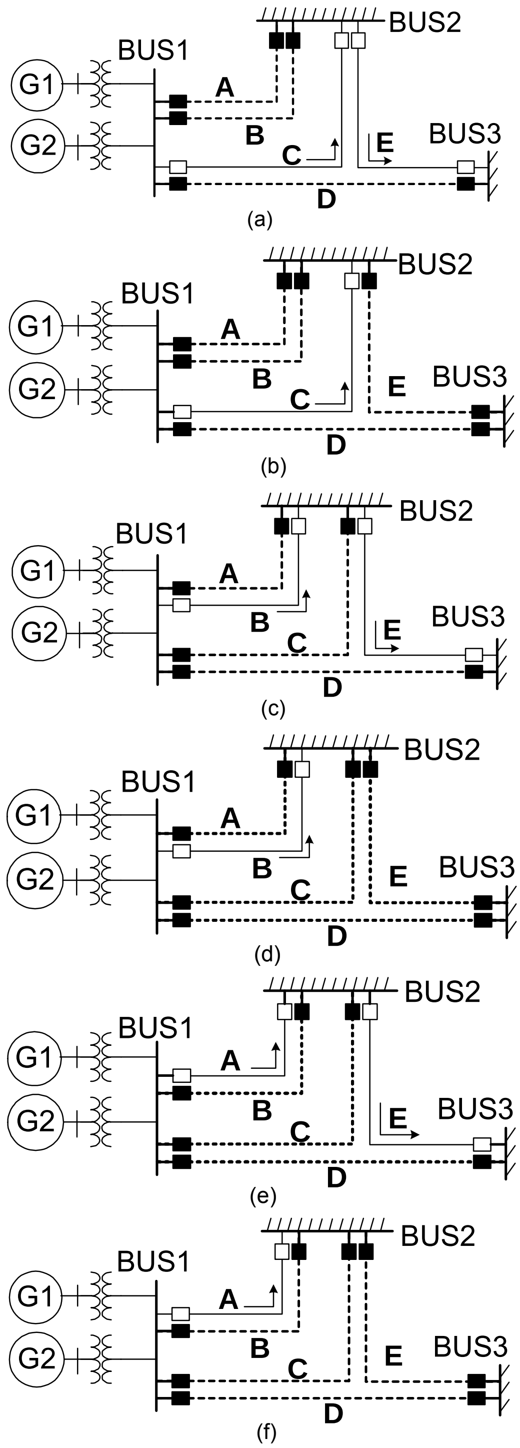

Fig. 11. N-3 conditions with long lines being opened (a) Case 3-2A (circuits A, B, and D being opened), (b) Case 3-2B (circuits A, B, D, and E being opened), (c) Case 3-3A (circuits A, C, and D being opened), (d) Case 3-3B (circuits A, C, D, and E being opened), (e) Case 3-4A (circuits B, C, and D being opened), (f) Case 3-4B (circuits B, C, D, and E being opened).

[26] P. P. Bedekar, S. R. Bhide, and Vijay S. Kale, “Optimum Time Coordination of Overcurrent Relays in Distribution System Using Big-M (Penalty) Method”, WSEAS Trans. on Power Systems, vol. 4, no. 11, pp. 341-350, 2009.
[27] I. Yilmazlar and G. Kokturk, “Failure Analysis in Power System by the Discrete Wavelet Transform”, WSEAS Trans. on Power Systems, vol. 5, no. 3, pp. 243-252, 2010.
[28] A. F. B. Abidin, A. Mohamed, H. Shareef, “A New Detection Technique for Distance Protection during Power Swings”, Proceedings of the 9th WSEAS International Conference on Applications of Electrical Engineering, 2010.
[29] Z. Chen, F. Li, L. Fan, and P. Zhang, “Review of PMU-based Online Applications for Dynamic Simulation, Fault Detection, and Cascading Failure Prevention”, Proceedings of the 8th WSEAS International Conference on Electric Power Systems, High Voltages, Electric Machines (POWER '08), pp. 212-216, 2008.

Biographies

Chi-Jui Wu received the B. Sc., M. Sc., and Ph.D. degree in electrical engineering all from the National Taiwan University in 1983, 1985, and 1988, respectively. In 1988, he joined the Department of Electrical Engineering, National Taiwan University of Science and Technology as an associate professor. Now he is a full professor. He has been active in practical problems and got many projects from private companies, independent research institutes, and governments. His current research interests lie in electric power quality, power electromagnetic interference, and power system stability.

Ping-Heng Ho was born in Taiwan, R.O.C. in 1968. He received the B. Sc. and M. Sc. degrees in Information Management Department from the Ming Chuan University, Taipei, Taiwan, R.O.C., in 1999 and 2001, respectively. He is currently a Ph. D. student in the Electrical Engineering Department, National Taiwan University of Science and Technology. He has been with the Taiwan Power Company since 1993. Currently, he is a senior engineer in the System Planning Department, Taiwan Power Company. His major research fields are system analysis, network planning, and problem identification in electrical power systems.